International Journal of Modern Manufacturing Technologies
ISSN 2067–3604, Vol. XVII, No. 3 / 2025
https://doi.org/ 10.54684/ijmmt.2025.17.3.194

ELASTIC CONTACT SOLVER BASED ON PRESSURE DECONVOLUTION

Sergiu Spinu[1]

[1] Department of Mechanics and Technologies, Stefan cel Mare University of Suceava,
13th University Street, 720229, Romania

Corresponding author: Sergiu Spinu, sergiu.spinu@fim.usv.ro

Abstract: Fourier analysis has been extensively used for the solution of numerous contact problems, one chief application being the rapid computation of convolution products. This type of operation appears in contact modelling every time superposition of effects is applied. Elastic displacement in a contact process can be modelled as the superposition of effects of point forces acting normally on the half-space boundary. Applying discretisation and assuming the pressure as piece-wise constant, a semi-analytical formulation for the displacement equation can be achieved using influence coefficients. The resulting equation is a discrete convolution product, in which pressure can be regarded as the unknown if a numerical displacement is provided. The pressure derivation by deconvolution from the displacement equation can be efficiently performed in the Fourier domain on the condition that the periodicity error perturbing the outcome of non-periodic contacts is controlled. An expansion of the original domain for which pressure is needed, is proven by numerical simulation to reduce the periodicity error. Numerical examples are presented providing method validation by comparison with analytical results existing in the literature. A practical use of the method is then given, in the form an elastic contact solver based on energy minimization. The advanced computer code is validated by simulating the Hertz point contact and the surface cylindrical contact with load eccentricity. In all cases, the numerical predictions match the analytical curves. The program execution time of the new code is then benchmarked against the state-of-the-art from the literature. It is found that, for a specific choice of the ratio between the target and the computational domain, the new code can be faster in the tilting contact case, and does not fall far behind for the rest of the contact cases. The conducted simulations suggest that the new computer code is a valuable alternative to existing contact algorithms.

Key words: elastic contact, semi-analytical method, deconvolution, contact pressure.

1. INTRODUCTION

Computational complexity is the chief challenge in computational contact mechanics, with several types of contact problems considered unsolvable simply because of their complexity. In this context, Fourier analysis emerged as a necessary tool to reduce this computational complexity. The calculation of elastic displacement using Fourier analysis started with the pioneering works of these authors [1-3]. The acceleration of computation of convolution products that appear in all contact mechanics models was an important innovation that revolutionized the numerical treatment of the contact problems. The error free calculation of discrete cyclic convolutions using special techniques of domain manipulation and extension [4,5] encouraged the addition of additional nested iterative schemes that allowed the simulation of more complex material behavior, such as elastic-plastic [6,7] or viscoelastic [8,9]. Semi-analytical methods appeared as a new branch of numerical methods specifically designed for contact mechanics, having as strong points existing analytical solutions for the elastic half-space and the Fourier domain calculation of convolutions. As pointed out in [10], the semi-analytical algorithms necessitate, for the solution of a 3D contact problem, the same amount of computational resources as a finite element analysis for a 2D simulation. The difference stems from semi-analytical methods only meshing a close vicinity of the initial contact zone, but also from the efficiency of the Fast Fourier transform (FFT) in derivation of the discrete Fourier transform. Wang et al. [11] reviewed the various applications of FFT to computational contact mechanics.

Any contact mechanics algorithm is centered around a scheme iterating the contact area and the distribution of contact stresses. This is the outer loop of any contact process, and various nested loops can be added to model more complicated material behavior. Having a robust scheme for the assessment of the contact parameters is of paramount importance, and important research efforts, reviewed in [12], aimed for the optimal solution.

This paper explores a new elastic contact solver build around an energy minimization technique and taking advantage of the derivation of pressure by deconvolution from the displacement relation. The predictions of the

developed computer program are corroborated with the Hertz explicit solution. Simulation execution times are then benchmarked against algorithms from the literature. It is found that the new code is nearly as fast as the reference, and is particularly efficient when dealing with contact with load eccentricity.

2. MATERIALS AND METHODS

The main advantage of the semi-analytical treatment of contact problems is the use of the half-space assumption that promotes fundamental solutions describing the response of a semi-infinite body to boundary point loads. These theoretical solutions are mathematical idealisations (no point load can be obtained or applied in practical applications) upon which a partially analytical framework can be achieved, whose predictions agree well with existing analytical solutions. For contact problems in which friction is neglected, also referred to as normal contact problems, the relevant fundamental solution is the elastic displacement u_3 in a point of coordinates $(x_1, x_2, 0)$, due to a point load along the x_3- direction, applied at $(0,0,0)$. With the x_1 and x_2 directions contained in the half-space boundary, and the x_3-direction pointing inwards the body, the Green's function $G(x_1, x_2)$ becomes:

$$G(x_1, x_2) = u_3(x_1, x_2, 0) = \frac{1-\nu^2}{\pi E} \frac{1}{\sqrt{x_1^2 + x_2^2}}, \tag{1}$$

with ν and E the elastic parameters, i.e., the Poisson's ratio and the Young modulus, respectively. By replacing the point force with a distributed surface pressure, relation (1), derived by Boussinesq, cited in [13], can be integrated over the boundary to express the displacement due to an arbitrary pressure $p(x_1, x_2)$:

$$u_3(x_1, x_2) = \int_{-\infty}^{\infty} \int_{-\infty}^{\infty} p(\xi, \eta) G(x - \xi, y - \eta) d\xi d\eta . \tag{2}$$

Relation (2) is mathematically a (continuous) convolution product that cannot be expressed in closed form without assuming a specific form of *p*. To overcome this, discretization is applied, and the continuous pressure is replicated by cuboidal pressure elements of different heights that are factored out of (2), and only the integration of the Green's function (1) over the rectangular elementary cell remains to be solved. The latter was achieved analytically by Love, cited in [13]. By replacing the coordinates-based notation with integers positioning the referred elementary cell inside the grid, one can obtain the displacement $K(i-k, j-l)$ observed in the (i, j) elementary cell of area $\Delta = \Delta_1 \Delta_2$, due to a unity pressure uniform over the cell (k, l):

$$K(i-k, j-l) = \int_{x_2(l)-\Delta_2/2}^{x_2(l)+\Delta_2/2} \int_{x_1(k)-\Delta_1/2}^{x_1(k)+\Delta_1/2} G\left(x_1(i) - x_1', x_2(j) - x_2'\right) dx_1' dx_2' . \tag{3}$$

Here, $x_1(k)$ and $x_2(l)$ are the coordinates of the center of the (k, l) patch, and $x_1(i)$ and $x_2(j)$ those of the (i, j) cell. Relation (3) allows computing a 2D matrix of so called influence coefficients $K(i, j)$, which describe the influence of pressure in each elementary cell to displacement in every grid cell:

$$K(i,j) = \frac{1-\nu^2}{\pi E} \begin{pmatrix} f(x_1(i) + \Delta_1/2, x_2(j) + \Delta_2/2) + f(x_1(i) - \Delta_1/2, x_2(j) - \Delta_2/2) ... \\ -f(x_1(i) + \Delta_1/2, x_2(j) - \Delta_2/2) - f(x_1(i) - \Delta_1/2, x_2(j) + \Delta_2/2) \end{pmatrix}, \tag{4}$$

with the assistance of the dummy function:

$$f\left(x_1, x_2\right) = x_1 \ln\left(x_2 + \sqrt{x_1^2 + x_2^2}\right) + x_2 \ln\left(x_1 + \sqrt{x_1^2 + x_2^2}\right). \tag{5}$$

Substituting the infinite limits of integration in (2) with a discrete set of rectangular surface patches A_p, i.e. a computational discretized domain, one can obtain the discrete counterpart of (2) as:

$$u_3(i,j)=\sum_{(k,l)\in A_P}\left(p(k,l)\int_{x_2(l)-\Delta_2/2}^{x_2(l)+\Delta_2/2}\int_{x_1(k)-\Delta_1/2}^{x_1(k)+\Delta_1/2}G\left(x_1(i)-x_1',x_2(j)-x_2'\right)dx_1'\,dx_2'\right)=\sum_{(k,l)\in A_P}p(k,l)K\left(i-k,j-l\right),\quad(6)$$

which is also a convolution product, but discrete. Relation (6) can be calculated for arbitrary (digitized) pressure and can be regarded as a semi-analytical counterpart of (2) because, although discretisation of pressure distribution is imposed, analytical integration is achieved in the expression of the influence coefficients matrix.
Moreover, the calculation of (6) can benefit from specialized numerical techniques derived specifically for these type of multiplications. The state-of-the-art method recognized in the literature is the Discrete Convolution Fast Fourier Transform (DCFFT) [4,5]. The main idea of the algorithm is to perform the calculation of the discrete convolution (6) in the frequency domain, supported by the convolution theorem, which states that, for two arbitrary functions $p(\tau)$ and $g(\tau)$:

$$\int_{-\infty}^{\infty}p(\tau)g(t-\tau)d\tau\equiv IFT(FT(p)\cdot FT(g)),\quad(7)$$

with *FT* denoting the direct and *IFT* the inverse Fourier transforms. Relation (7) holds true for discrete multidimensional convolutions such as (6) if the Fourier transforms are replaced by fast Fourier transforms *FFT* and *IFFT*, and the matter of the periodicity error [4] is addressed. Thus, by applying (7) to relation (6):

$$u_3=IFFT(FFT(p)\cdot FFT(K)).\quad(8)$$

The displacement equations (6) or (8) can be regarded as equations in *p* if the displacement field u_3 is known in numerical form. Thus, an inverse problem can be formulated: obtain the pressure that induces a known displacement field. In this situation, pressure is deconvoluted from the displacement equation, so that from (8):

$$p=IFFT\left(\frac{FFT(u_3)}{FFT(K)}\right).\quad(9)$$

The literature has proven [5] that the direct application of (8) to the calculation of (6) introduces errors that can be minimized or completely eliminated by an extension of the problem domain. The periodicity error was explained in the literature in the following manner: whereas *p* is generally non-periodic (but can be assumed periodic in statistical models for nominally flat contact geometry), $FFT(p)$ implies periodicity. Thus, the displacement calculated from (8) is the sum of contributions of multiple adjacent pressure distributions. This error can be completely removed if the calculation is performed on a domain larger than the original one, with pressure that is zero-padded in the extended region. Conceptually, one can think that the false pressure periods introduced by periodisation are moved farther away due to the zero-padded region, and thus the interference is minimized or eliminated.
Given the aforementioned problem periodisation by application of *FFT*, it is expected that the pressure deconvoluted from (9) is also affected by the periodicity error. Numerical simulations are performed to check the validity of relation (9) as a means to compute pressure from known displacement. To this end, the Hertz point contact framework is used, featuring one of the few existing closed form expressions for both pressure and the associated displacement, *r* being the radial coordinate:

$$p(r)=p_H\sqrt{1-\left(\frac{r}{a_H}\right)^2},\quad(10)$$

$$u_3(r)=\begin{cases}\pi\eta p_H\dfrac{2a_H^2-r^2}{2a_H},\ |r|\le a_H;\\ \eta\dfrac{p_H}{a_H}\left[(2a_H^2-r^2)\sin^{-1}(a_H/r)+ra_H\sqrt{1-\left(a_H/r\right)^2}\right],\quad |r|>a_H,\end{cases}\quad(11)$$

with a_H, p_H and η the contact radius, the maximum central pressure, and the contact compliance, respectively. A target and a computational domains were established, both square, of side lengths $L_0 = 2a_H$ and L. Relations (11) and (4) were used to generate numerical data for both u_3 and K in the computational domain, then equation (9) gave the pressure predicted for the target domain. The impact of the ratio L/L_0 on the calculated radial pressure is depicted in figure 1.

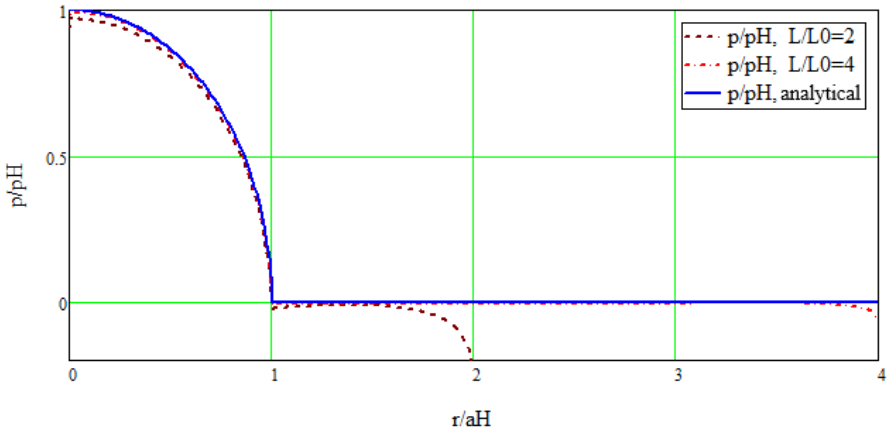

a)

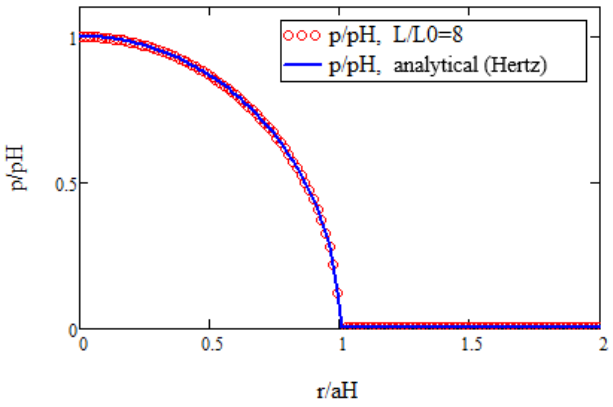

b)

Fig. 1. Pressure profiles obtained by deconvolution: a) $L/L_0 \le 4$; b) $L/L_0 = 8$.

The numerical predictions depicted in figure 1 suggest that a domain extension of $L/L_0 = 8$ or $L/L_0 = 4$ (in every direction) provides good precision in the domain on interest. The most important errors in these cases are located near the boundary (see the vicinity of $r/a_H = 4$ in figure 1.a), which is not of interest as pressure is needed only in the target domain $|r| \le a_H$. Some feeble deviations from the theoretical Hertz profile can also be spotted even for $L/L_0 = 4$, whereas $L/L_0 = 2$ is found to be lacking precision everywhere. The case $L/L_0 = 8$ appears to follow closely the theoretical curve in a domain twice the target one, as concluded from figure 1b.
The calculation of pressure inducing an arbitrary numerical displacement field can thus be performed based on relation (9) with a $L/L_0 \ge 4$ ratio. The use of this findings in a contact solver featuring pressure deconvoluted from numerical displacement is explored next.
Kalker and van Randen [14] formulated the elastic contact problem as problem of minimization of energy. According to this formulation, for a contact process, complementary energy V and its gradient can be expressed as:

$$V(\mathbf{p}) = \frac{1}{2}\mathbf{p}^{\mathrm{T}}\mathbf{K}\mathbf{p} - \mathbf{p}(\omega - \mathbf{hi}), \quad \mathbf{V}'(\mathbf{p}) = \mathbf{K}\mathbf{p} - (\omega - \mathbf{hi}), \tag{12}$$

while the potential energy and its gradient:

$$E(\mathbf{h}) = \frac{1}{2}\mathbf{h}^{\mathrm{T}}\left(\mathbf{K}^{-1}\right)\mathbf{h} + \mathbf{h}^{\mathrm{T}}(\omega - \mathbf{hi}), \quad \mathbf{E}'(\mathbf{h}) = \left(\mathbf{K}^{-1}\right)(\mathbf{h} + \omega - \mathbf{hi}). \tag{13}$$

In relations (12) and (13), the following notations are used: **h** - the gap between the deformed contacting surfaces, ω - the rigid-body approach, and **hi** - the gap between the undeformed contacting surfaces. Bold parameters denote matrix-vector notation. A solution of the system (12) and (13) can be sought either by minimizing **h** over the contact area, on condition that **p** is nil in the non-contact region, or by minimizing **p** on condition that **h** is nil over the contact area. Both formulations are quadratic minimization schemes whose convergence is guaranteed. The first route is referred to as the method of complementary energy, and the second the method of potential energy. Based on this framework, an energy minimization scheme is advanced in this paper, based on an idea originally proposed by Kawabata and Nakamura [15]. The steps of the algorithm are described below:

1. Import contact geometry **hi**, the properties of the contacting materials, ν and E, for each contacting body, and the load transmitted through the contact, W.
2. Establish a target domain expected to encompass the contact area, as well as a computational domain according to the pressure deconvolution method described in the previous section. Choose the number of grids in each direction, and then compute the matrix **K** of influence coefficients in the computational domain according to (4).
3. Set the initial values $\mathbf{h} = \mathbf{0}$ and $\omega = 0$.

The following instructions run in a loop:

4. Compute the elastic displacement field according to the geometrical condition of deformation:

$$\mathbf{u}_3 = \mathbf{h} - \mathbf{hi} + \omega, \tag{14}$$

5. Use this displacement to obtain pressure by deconvolution according to relation (9).
6. The resulting **p** satisfies (14) but may exhibit negative values in some grid points, which is not convenient because adhesion is not accounted for in the contact model. To correct this, uniform pressure δp is added on the discrete contact area A_P, so that the static force equilibrium is verified, i.e. W is balanced by **p**:

$$\Delta\sum_{(i,j)}\left(p(i,j) + \delta p\right) = W, \quad (i,j) \in \left\{(i,j) \in A_P, p(i,j) + \delta p > 0\right\}, \tag{15}$$

$$\mathbf{p} \leftarrow \mathbf{p} + \delta p. \tag{16}$$

7. Set negative nodal pressures to zero:

$$p(i,j) = 0, \quad (i,j) \in \left\{(i,j) \in A_P, p(i,j) < 0\right\}. \tag{17}$$

8. Recompute the current displacement field using relation (8). This calculation is best performed assisted by DCFFT [4,5].
9. Recompute the current gap along the normal direction, measured between the profiles of the deformed bodies:

$$\mathbf{h} = \mathbf{u}_3^{pr} + \mathbf{hi} - \omega. \tag{18}$$

10. The current solution has minimal potential energy, but the gap **h** does not vanish over the contact area. Moreover, existing negative pressure elements are not consistent with the of linear Theory of Elasticity, which does not allow penetration of bodies. To correct this, uniform displacement is added so that the gap on the contact boundary vanishes:

$$h \leftarrow h + \frac{\sum_{(i,j)\in I_C} u_3(i,j) + hi(i,j)}{\mathrm{card}(I_C)}, \quad I_C = \left\{(i,j) \in A_P, p(i,j)p(i,j+1) < 0 \vee p(i,j)p(i+1,j) < 0\right\}, \tag{19}$$

11. Set negative **h** to zero:

$$h(i,j)=0, \quad (i,j)\in\{(i,j)\in A_P, h(i,j)<0\}. \tag{20}$$

The loop breaks when either all nodal pressures $p(i,j)$ or all nodal gaps $h(i,j)$, are positive or zero. A mean value calculated over the cells with negative pressure or with negative gap can serve as criterion of convergence. The described contact model can equally treat the situation of tilting moment inducing the rotation of the common plane of contact. To this end, the pressure corrector δp in step (15) should not be uniform, but varying linearly with coordinates. A Mathcad computer code was created based on the framework described in this paper, and its predictions were benchmarked against the classic elastic contact solver advanced by Polonsky and Keer [16]. The results are presented in the following section.

3. RESULTS AND DISCUSSIONS

Numerical simulations were performed for both the non-conforming and the conformal contact. From the first category, a Hertz point contact between was chosen. The numerical predictions agree well with the theoretical curve, as shown in figure 2, in which the Hertz contact parameters a_H and p_H were used as normalizers.

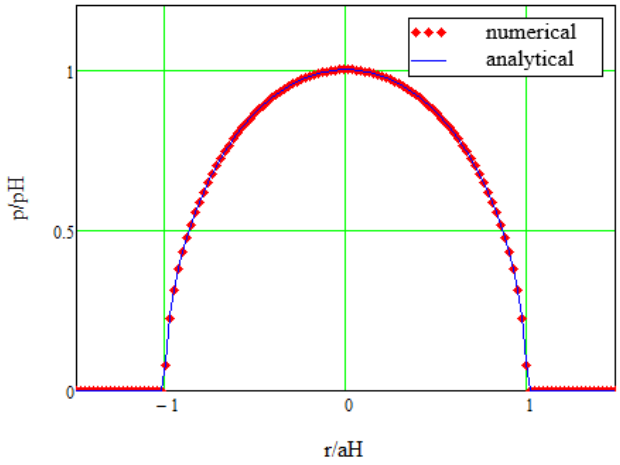

Fig. 2. Computer code validation for the Hertz point contact.

A good agreement was also observed for the conformal contact. A cylinder of radius *R* was pressed with a force aligned with the cylinder axis against a half-space. For this scenario, a load eccentricity *e* along the x_1-direction was introduced, causing the tilting of the common plane of contact with a minute angle. The closed form analytical solution for this contact case is given in [17]. Figure 3 shows a good match between literature and the numerical predictions.

The computational performance of the advanced computer program was then assessed against the classical algorithm proposed by Polonsky and Keer [16]. The original scheme, designed around the Conjugate Gradient method, did not take into account tilting moments. These authors [18] extended the algorithm, and the modified version is used for comparison.

Figure 4 show in percents the computational time of the new computer code versus the classical one, which, for each contact case, is set as reference (i.e., 100%). In each simulation, the ratio L/L_0 between the target and the computational domain was varied. According to the data from figure 1, smaller L/L_0 provides less precision in the pressure deconvolution sequence, resulting in slower convergence in the contact solver. As opposed to larger L/L_0, which require more computational resources but speed up the convergence of the contact solver due to better precision. Similar precision goals were imposed in both the classical and the new computer code.

The results depicted in figure 4 suggests that the total program execution time favors the choice $L/L_0=4$, which provide execution times similar to those of the classical algorithm, whereas the ratio $L/L_0=8$ results in inefficiency. In should also be noted that, doubling the ratio L/L_0 results in quadrupling the memory requirement. There exists an instance in which the computational time of the classical algorithm has been beaten, namely the case with eccentric loading and $L/L_0=4$.

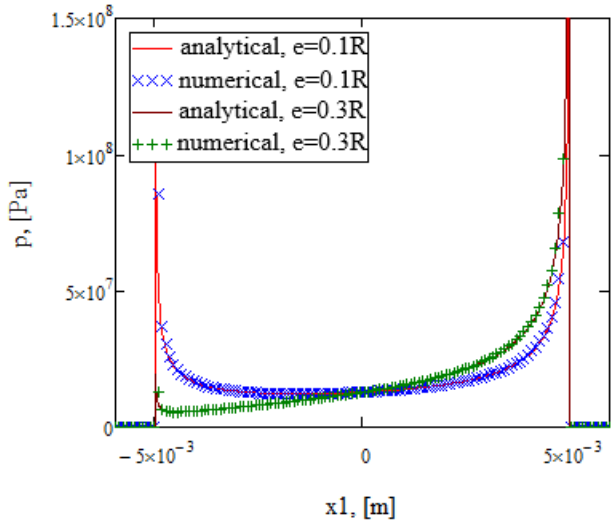

Fig. 3. Computer code validation for the conformal eccentric contact.

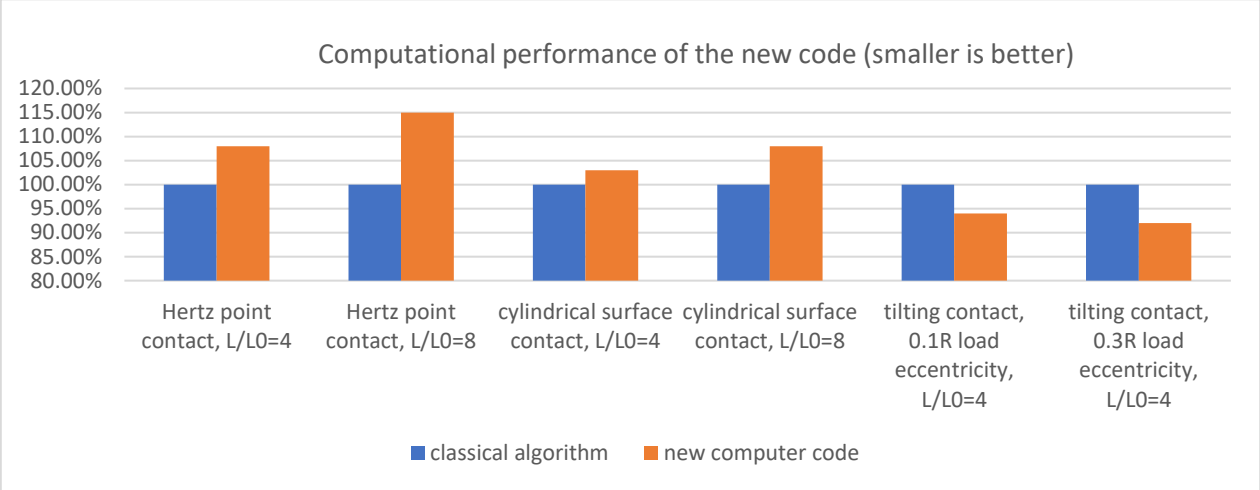

Fig. 4. Program execution times (in percentage of the classical algorithm).

4. CONCLUSIONS

The semi-analytical solving of elastic contact problems is a subject of interest because others numerical approaches, such as finite element analysis, lead to prohibitive computational times. The mathematical model treatment using Fourier analysis is a modern trend relying on the convolution theorem and on its ability to dramatically improve the computational times of convolution products.

An inverse problem is considered in this paper, aiming to derive the pressure that induces a known, but otherwise arbitrary, numerical displacement. The unknown pressure is derived in the frequency domain for computational efficiency, assisted by the convolution theorem. The deconvoluted pressure exhibits errors related to the periodicity error associated with the implicit periodisation of problem parameters. These errors can be reduced by performing the deconvolution in a domain larger than the domain of interest. As this requires more computational resources, the optimal choice of the domain extension ratio is a matter of numerical experimentation.

Besides its theoretical value, the deconvolution procedure has direct applicability in the solution of the elastic contact problem with arbitrary geometry. An energy minimization scheme advanced in the literature is employed to solve the contact problem, with the pressure deconvolution as an important step of the algorithm.

The predictions of the resulting computer code are first validated by comparison with analytical results from the theory of Contact Mechanics. The validation included the Hertz point contact and the surface contact between a cylinder and a flat. To increase generality, in the latter case, the tilting of the common plane of contact was also simulated. In all scenarios, program predictions matched well the analytical curves.

Comparison of program execution times with the state-of-the-art based on the Conjugate Gradient method revealed that the newly proposed computer code was nearly as fast with a specific choice of the domain extension ratio. Encouraging program execution times were attained for the tilting contact scenario, in which the new code proved to be faster with up to 15%.

Author contributions: The author confirms the sole responsibility for the conceptualization of the study, methodology, creation of new software used in the paper, validation and visualization of presented results, and manuscript preparation, review and editing.
Funding source: This paper has received no external funding.
Conflicts of interest: There is no conflict of interest.

5. REFERENCES

1. Ju, F., Farris, T. N., (1996). *Spectral Analysis of Two-Dimensional Contact Problems*, ASME J. Tribol. 118(2) 320-328.
2. Ju, F., Farris, T. N., (1997). *FFT Thermoelastic Solution for Moving Heat Sources*, ASME J. Tribol. 119(1) 156-162.
3. Stanley H. M., Kato, T., (1997). *An FFT-Based Method for Roughness Surface Contact*, ASME J. Tribol. 119 493-500.
4. Liu, S. B., Wang, Q., and Liu, G., (2000). *A Versatile Method of Discrete Convolution and FFT (DC-FFT) for Contact Analyses*, Wear 243(1–2) 101–110.
5. Liu, S., Wang, Q., (2001). *Studying Contact Stress Fields Caused by Surface Tractions with a Discrete Convolution and Fast Fourier Transform Algorithm*, ASME J. Tribol. 124 36-45.
6. Jacq, C., Nelias, D., Lormand, G., Girodin, D., (2002). *Development of a Three-Dimensional Semi-Analytical Elastic-Plastic Contact Code*, ASME J. Tribol. 124 653-667.
7. Nélias, D., Antaluca, E., Boucly, V., and Crețu, S., (2007). *A Three-Dimensional Semianalytical Model for Elastic-Plastic Sliding Contacts*, ASME J. Tribol. 129 761 – 771.
8. Chen, W. W., Wang, Q. J., Huan, Z., and Luo, X., (2008). *Semi-Analytical Viscoelastic Contact Modeling of Polymer-Based Materials*, ASME J. Tribol., 133(4), 041404.
9. Spinu, S., Cerlinca, D., (2016). *A Robust Algorithm for the Contact of Viscoelastic Materials*, IOP Conference Series: Materials Science and Engineering, 145(4) 042034.
10. Renouf, M., Massi, F., Fillot, N., and Saulot, A., (2011). *Numerical Tribology of a Dry Contact*, Tribol. Int., 44(7), pp. 834–844.
11. Wang, Q. J., Sun, L., Zhang, X., Liu, S., and Zhu, D., (2020). *FFT-Based Methods for Computational Contact Mechanics*, Front. Mech. Eng. 6 61.
12. Allwood, J. M., (2005). *Survey and Performance Assessment of Solution Methods for Elastic Rough Contact Problems*, ASME J. Tribol. 127 10-23.
13. Johnson K. L., (1985) Contact Mechanics (Cambridge: University Press).
14. Kalker, J. J., Van Randen, Y., (1972). A Minimum Principle for Frictionless Elastic Contact with Application to Non-Hertzian Half-Space Contact Problems", J. Eng. Math. 6(2) 193-206.
15. Kawabata, S., Nakamura, T., (2003). *New Iteration Method for FFT Based Contact Analysis*, Proc. of 2003 STLE/ASME Joint International Tribology Conference, Ponte Vedra Beach, Florida USA.
16. Polonski, I. A., Keer, L. M., (2000). *A Fast and Accurate Method for Numerical Analysis of Elastic Layered Contacts*, ASME J. Tribol. 122(1) 30.
17. Lurie, A. I., (1964). Three Dimensional Problems of the Theory of Elasticity (Interscience Publishers).
18. Spinu, S., Diaconescu, E., (2008). *Numerical Simulation of Elastic Conforming Contacts under Eccentric Loading*, Proceedings of the STLE/ASME International Joint Tribology Conference, Miami, Florida, USA

Received: July 22th, 2025 / Accepted: November 12th, 2025 / Paper available online: December 20th, 2025